Parameter Optimization of PID Sliding Mode Controller for Hydraulic Turbine Regulating System Based on IFABC Algorithm

Gonggui Chen, Xiaoxia Tan, Zhizhong Zhang*, and Zhi Sun

Abstract— **Hydraulic turbine regulating system (HTRS) is a complex and nonlinear system, which might not be controlled well by traditional PID controller. Fortunately, sliding mode controller (SMC) has certain advantages in dealing with nonlinear system. Moreover, the design of control law for controller is difficult but extremely necessary. Therefore, an improved fuzzy artificial bee colony algorithm (IFABC) is proposed and applied to the parameter optimization of improved PID-SMC (IPID-SMC) controller, which will be compared with the conventional PID controller and traditional SMC controller. The simulation results indicate that the proposed IPID-SMC controller improves the nonlinear HTRS system performance with faster convergence speed and accurate convergence precision. In the proposed method, the sliding surface of the controller has been integrated with proportional-integral-derivative (PID) controller, and the parameters of PID controllers first obtained through particle swarm optimization (PSO) algorithm. Next, other parameters will be optimized by these four algorithms, which include DE algorithm, PSO algorithm, ABC algorithm and IFABC algorithm. The results show that the proposed IFABC algorithm reduces the chattering of IPID-SMC controller and improves the dynamic performance of the nonlinear HTRS system.**

Index Terms— **Hydraulic Turbine Regulating System (HTRS), Sliding Mode Controller (SMC), PID Sliding Surface, Improved PID Sliding Mode Controller (IPID-SMC), Improved Fuzzy Artificial Bee Colony Algorithm (IFABC)**

I. Introduction

Hydraulic turbine regulating system (HTRS) is a non-minimum phase and complex nonlinear system, which is composed of conduit system, water turbine system, servo system and generator system [1-4]. In the electrical power system, the instability of the client load will cause the safety and quality problems of the users. Therefore, the optimization of the dynamic performance of HTRS system is especially important. Establishing a suitable control rule for HTRS system is still a serious problem due to the nonlinear characteristics and varying loads [5-7].

In recent years, PID controller [8] is widely used in the dynamic performance optimization of HTRS system because of its simple structure and easy implementation [9, 10]. However, the PID controller is too simple to handle signals and does not take full advantage of it. In the past decades, more and more advanced controller is designed for HTRS system, such as robust controller, integrated management controller (IMC), fuzzy controller, load shedding controller and sliding mode controller (SMC), etc. Among them, SMC controller is applied to optimize the dynamic performance of the HTRS system due to its rapid response, online monitoring, simple implementation and strong robustness [11].

SMC controller is essentially a special kind of nonlinear control whose nonlinearity is represented by the discontinuity of the control [12]. Different from other control strategies in that the 'structure' of system is not fixed, and the destination is constantly changing in the dynamic process according to the current state of the system, finally the system is forced to move to a predetermined state trajectory. In Refs. [13, 14], the first-order SMC controller and second-order SMC controller is adopted to turning the dynamic performance of HTRS system when it is under the load and frequency conditions, respectively. The simulation results prove the effectiveness of SMC controllers in dominating HTRS system. However, it is worth noting that the hydropower systems previously involved are linear, and the robustness of the SMC controller in hydropower systems has not been proven for some of the external and uncertain disturbances.

In order to modify the shortcomings of the standard SMC controller, we proposed an improved SMC controller (IPID-SMC), which combines the PID control with sliding mode control. One of the key stages in establishing SMC control is the structural design of the sliding surface. On the one hand, due to the simple feasibility and wide application of PID control. On the other hand, in order to ensure that HTRS system track the frequency given value well, the proportional-integral-differential (PID) is taken as the sliding mode surface for SMC controller. Another key stage in the design of the SMC controller is the design of sliding mode control law. Among them, the robustness of the sliding mode control is guaranteed by the switching control, but the chattering of the sliding mode control is caused by the

Manuscript received October 15, 2018; revised December 10, 2018. This work was supported by Innovation Team Program of Chongqing Education Committee (CXTDX201601019), Chongqing University Innovation Team under Grant (KJTD201312) and the National Natural Science Foundation of China (Nos. 51207064 and 61463014).

Gonggui Chen is with the Key Laboratory of Industrial Internet of Things & Networked Control, Ministry of Education, Chongqing University of Posts and Telecommunications, Chongqing 400065, China; Key Laboratory of Complex Systems and Bionic Control, Chongqing University of Posts and Telecommunications, Chongqing 400065, China (e-mail:chenggpower@126.com).

Xiaoxia Tan is with the Key Laboratory of Industrial Internet of Things & Networked Control, Ministry of Education, Chongqing University of Posts and Telecommunications, Chongqing 400065, China. (e-mail: dimples_txx@163.com).

Zhizhong Zhang is with the Key Laboratory of Communication Network and Testing Technology, Chongqing University of Posts and Telecommunications, Chongqing 400065, China (corresponding author, Tel: 023-62461681; e-mail: zhangzztx@163.com).

Zhi Sun is with the Guodian Enshi Hydropower Development, Enshi 445000, China (e-mail: sunzhi24@126.com).

Nomenclature

Hydraulic Turbine Regulating System (HTRS):

♦ the Parameters of Hydro-turbine

M_t	the torque of the hydro-turbine	e_{mx}	the partial derivatives of hydro-turbine
Q	the water flow of the hydro-turbine	e_{my}	torque with respect to the hydro-turbine
m_t	the deviation of the hydro-turbine torque	e_{mh}	speed, guide vane and water head
q	the deviation of the hydro-turbine water flow		
x	the deviation of the hydro-turbine speed	e_{qx}	the partial derivatives of hydro-turbine flow
y	the deviation of the hydro-turbine guide vane	e_{qy}	with respect to the hydro-turbine speed,
h_t	the deviation of the hydro-turbine water head	e_{qh}	guide vane and water head
h_w	the characteristic coefficient of the pipeline		
u	the output of the controller	T_{ab}	the mechanical starting time
T_y	the relay related time constant		

♦ the Parameters of Generator

δ	the relative deviation of generator rotor angle	$x_{d\Sigma}$	the direct axis reactance of generator
ω	the relative deviation of generator speed	x'_d	the transient axis reactance of generator
D	the damping constant of generator	x_T	the short-circuit reactance of transformer
M_e	the electromagnetic torque of generator	x_L	the reactance of transmission lines
P_e	the electromagnetic power of generator	$x_{q\Sigma}$	the quadrature axis reactance of generator
E'_d	the transient voltage of d-axis	x_q	the synchronous of quadrature axis
V_s	the generator voltage of infinite bus system		

♦ the Parameters of Controller

• PID controller

K_p	the proportional adjustment coefficient
K_i	the integral adjustment coefficient
K_d	the differential adjustment coefficient

• SMC controller

s	the designed sliding mode surface
λ	a positive constant of sliding mode controller
η	a positive constant of assisted item
Δ	a small constant of sliding mode controller

• IPID-SMC controller

η_1	a constant of assisted item
η_2	a constant of assisted item
ξ	a small constant of IPID-SMC controller
K_p'	the proportional adjustment coefficient of IPID-SMC controller
K_i'	the integral adjustment coefficient of IPID-SMC controller
K_d'	the differential adjustment coefficient of IPID-SMC controller

switching control. For these reasons, the saturation function is used instead of the sign function to reduce chattering that come from SMC controller in Ref. [15]. However, the tracking accuracy and disturbance rejection characteristics will be reduce because of the limitation of sliding mode variable. The fuzzy method is added into the SMC controller design to decrease chattering in Ref. [16]. However, there are some issues for the fuzzy idea. Firstly, the fuzzy control rules are mostly based on the experience of experts or the existing knowledge of people, and different people possess different fuzzy control rules. Secondly, the acquisition of fuzzy SMC controller parameters requires long-term and extensive trial and error, which is unlikely to be realized in practical applications. In Ref. [17], the SMC controller is designed by combining the proportional-differential and sliding surface, but there is still a strong chattering.

In this paper, a novel PID-SMC controller is proposed to reduce the chattering of traditional SMC controller and improve the ability to resist external interference, so that the dynamic performance and stability of nonlinear system are improved. At the same time, the switching function is modified by adding a new term and introducing a new continuous function. Among them, the proportions, integrals and differential coefficients that obtained from experience or other articles are unable to satisfy the accuracy of designing controller, so the intelligent algorithms will be used to optimize these three coefficients, which will be applied to design the IPID-SMC controller.

Fortunately, the application of various artificial intelligence algorithms will solve the above problems effectively. In Refs. [18, 19], SMC controllers based on particle swarm optimization (PSO) and imperialism competitive algorithms (ICA) are applied to solve the nonlinear problems in HTRS system. However, there are some problems of two kinds of algorithms, which include that are prone to local optimum and poor convergence, it is also difficult for fuzzy sliding mode controller to obtain more accurate parameters. The artificial bee colony algorithm (ABC) is a bionic intelligent evolutionary algorithm (EA) that has developed rapidly in recent years [20]. The algorithm searches for high-quality solutions by simulating bee foraging activities. What's more, the algorithm will perform global exploration and local exploitation during each iteration. This is also the difference between ABC algorithm and other intelligent algorithms such as PSO algorithm [21, 22], differential evolution algorithm (DE), and cuckoo search

algorithm [23, 24], but there are also some problems such as low optimization accuracy and poor convergence. Therefore, this paper proposes an improved fuzzy artificial bee colony algorithm (IFABC), which based on standard ABC algorithm.

The rest of the paper is organized as follows: In Section II, a nonlinear dynamic model of HTRS system is introduced, which include conduit system, water turbine system, electric hydraulic servo system and generator system. Section III introduces the working process of SMC and IPID-SMC controller. Section IV summarizes the ABC algorithm and describes the proposed IFABC algorithm in detail. And then the structure diagram of IPID-SMC controller assisted with IFABC algorithm for HTRS system is proposed in Section V. The simulations and analysis are given in Section VI. Finally, Section VII draws conclusions of this paper.

II. A Nonliinear Dynamic Model

The structure of HTRS system is illustrated in Fig. 1.It can be seen from Fig. 1, the HTRS system is mainly composed of conduit system, water turbine system, electro-hydraulic servo system and generator system [1-4].

A. Mathematical Model of Conduit System

The conduit system is significantly important to the unit's operation. And it is usually consists of water guiding tunnel, surge tank and pressure pipeline. The function of the system is to introduce the water flow of the upstream reservoir into the water conduit to promote the work of the generator unit.

The common linear model of turbine only considers rigid water hammers, but plastic water hammer is often an important factor that cannot be ignored in the theoretical research and engineering practice of HTRS system. Since both the water body and pipe wall are elastic, the effect of this elastic water hammer effect on the system must be taken into account when the pipe is so long. When considering more detailed nonlinear factors in the system, the transfer function between unit flows q to h is generally expressed as a hyperbolic section function as shown below.

$$G_h(s) = -2h_w th(0.5T_r s) \tag{1}$$

Where h_w is the characteristic coefficient of pipeline, T_r is the water hammer time constant of pipeline.

Expanding the above Eq. (1) into the following as:

$$G_h(s) = -2h_w \frac{\sum_{j=0}^{n} \frac{(0.5T_r s)^{2j+1}}{(2j+1)!}}{\sum_{i=0}^{n} \frac{(0.5T_r s)^{2i}}{(2i)!}} \tag{2}$$

Conduit system is rigid when n=0; and when n≥1, it is an elastic water hammer system. Therefore, when n=1, Eq. (2) can be written as follows.

$$G_h(s) = -2h_w \frac{\frac{1}{48}T_r^3 s^3 + \frac{1}{2}T_r s}{\frac{1}{8}T_r^2 s^2 + 1} \tag{3}$$

Further, we can obtain the transfer function between the guide vane and torque of HTRS system as follows.

$$G_t(s) = -\frac{e_{my}}{e_{qh}} \cdot \frac{e_m s^3 - \frac{3}{h_w T_r} s^2 - \frac{24}{h_w T_r^3}}{s^3 + \frac{3}{e_{qh} h_w T_r} s^2 + \frac{24}{T_r^2} s + \frac{24}{e_{qh} h_w T_r^3}} \tag{4}$$

Where e_m is an intermediate variable, and $e_m = e_{qy} * e_{mh} / e_{my} - e_{qh}$.

In conclusion, the state space equations of Eq. (4) can be shown as Eq. (5).

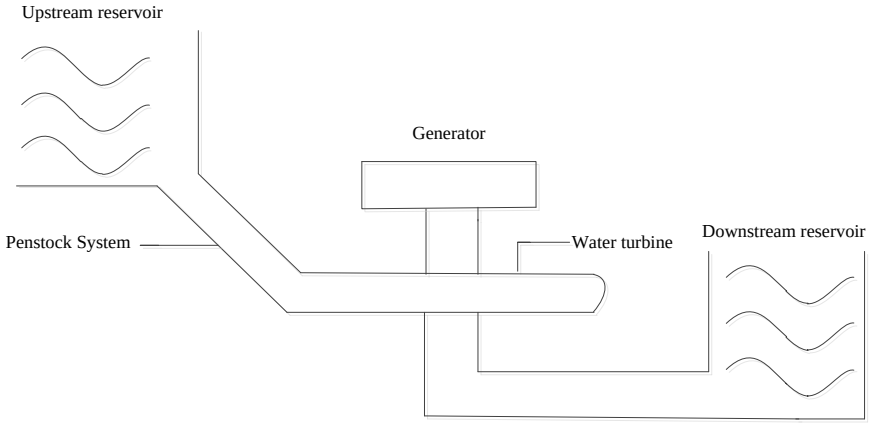

Fig. 1. A layout scheme of the hydro power station plant

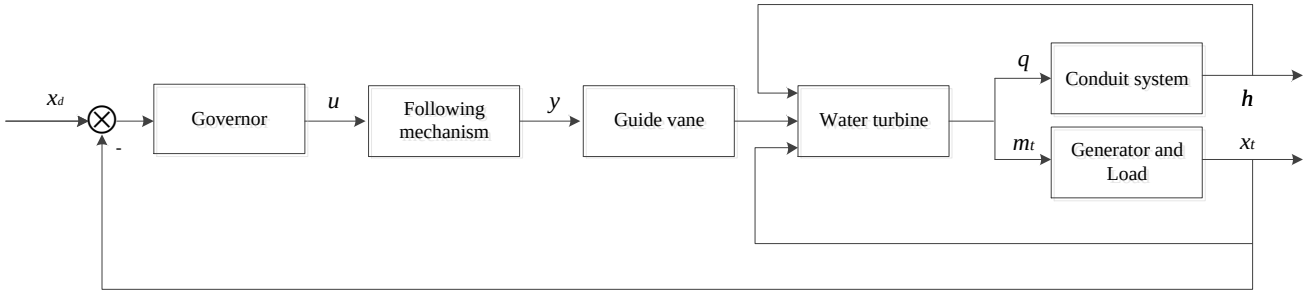

Fig. 2.The structure diagram of HTRS system

$$\begin{cases} \dot{x}_1 = x_2 \\ \dot{x}_2 = x_3 \\ \dot{x}_3 = -a_0 x_1 - a_1 x_2 - a_2 x_3 + y \end{cases} \tag{5}$$

Where $a_0 = \frac{24}{e_{qh} h_w T_r^3}$, $a_1 = \frac{24}{T_r^2}$, $a_2 = \frac{3}{e_{qh} h_w T_r}$. x_1, x_2 and x_3 are intermediate variables.

B. Mathematical Model of Water Turbine System

The water turbine is the key part of the research on the HTRS system, and the structure diagram of HTRS system is shown in Fig. 2. The dynamic characteristics of HTRS system can be described as a torque function and a flow function as follows.

$$\begin{cases} M_t = M_t(x, y, h_t) \\ Q_t = Q_t(x, y, h_t) \end{cases} \tag{6}$$

Where M_t and Q_t are torque and water flow of hydro-turbine x, y and h_t denote the hydro-turbine head, hydro-turbine speed and guide vane opening, respectively.

The Taylor series is used to expand the Eq. (6), the following expression is obtained as Eq. (7) through omitting the higher order terms above the second order.

$$\begin{cases} \Delta m_t = e_{mx}\Delta x + e_{my}\Delta y + e_{mh}\Delta h_t \\ \Delta q_t = e_{qx}\Delta x + e_{qy}\Delta y + e_{qh}\Delta h_t \end{cases} \tag{7}$$

Where Δm_t, Δq_t, Δx, Δy, Δh_t, denote the relative deviation of M_t, Q_t, x, y and h_t, respectively. And $e_{mx} = \partial m_t / \partial x$, $e_{mh} = \partial m_t / \partial h$, $e_{my} = \partial m_t / \partial y$, $e_{qx} = \partial q_t / \partial x$, $e_{qy} = \partial q_t / \partial y$, $e_{qh} = \partial q_t / \partial h$ denote the transfer coefficient of M_t to x, transfer coefficient of M_t to y, transfer coefficient of M_t to h, transfer coefficient of Q_t to x, transfer coefficient of Q_t to y, transfer coefficient of Q_t to h, respectively.

C. Mathematical Model of Electro-hydraulic Servo System

Electro-hydraulic servo system is the actuator of water turbine, which mainly acts on the controller. Simplified its model to a first-order system and expressed as follows.

$$T_y \frac{dy}{dt} + y = u \tag{8}$$

Where y, u represent the relay stroke and output of the controller, respectively. T_y is the time constant (s) associated with the relay.

D. Mathematical Model of Generator System

In order to understand the oscillation process and stability of the generator under the disturbance, a second-order generator model is adopted in this study. And the expression of generator can be represented as follows.

$$\begin{cases} \dot{\delta} = \omega_0 \omega \\ \dot{\omega} = \frac{1}{T_{ab}}(m_t - m_e - D\omega) \end{cases} \tag{9}$$

Where δ, ω, T_{ab} denote the rotor angle, the deviation of relative speed and generator mechanical time constant, respectively. And $\omega_0 = 2\pi f_0$, D stands for damping coefficient, which is generally regarded as a constant, and the value is between 0 and 3.

It is generally considered that the electromagnetic power P_e is equal to its electromagnetic torque m_e when analyzes the dynamic characteristics of the generator, which can be written as follows.

$$m_e = P_e \tag{10}$$

In a hydroelectric system, the electromagnetic power of the generator can be expressed as follows.

$$P_e = \frac{E'_d V_s}{x'_{d\Sigma}} \sin\delta + \frac{V_s^2}{2} \cdot \frac{x'_{d\Sigma} - x_{q\Sigma}}{x'_{d\Sigma} * x_{q\Sigma}} \tag{11}$$

Where E'_d is the transient voltage of d-axis in generator, $x_{q\Sigma}$ and $x'_{d\Sigma}$ denote the reactance sum of q-axis and d-axis, which are described as follows.

$$\begin{cases} x'_{d\Sigma} = x'_d + x_T + \frac{1}{2}x_L \\ x_{q\Sigma} = x_q + x_T + \frac{1}{2}x_L \end{cases} \tag{12}$$

Where x_T and x_L are the short-circuit reactance of transformer and the reactance of transmission lines, respectively.

E. Mathematical Model of HTRS System

In summary, the HTRS system is a multi-inputs and multi-outputs system, and the state-space equation for the HTRS system is described as follows.

$$\begin{cases} \dot{x}_1 = x_2 \\ \dot{x}_2 = x_3 \\ \dot{x}_3 = -a_0 x_1 - a_1 x_2 - a_2 x_3 + y \\ \dot{\delta} = \omega_0 \omega \\ \dot{\omega} = \frac{1}{T_a}\left(m_t - \frac{E_q' V_s}{x_{d\Sigma}'} \sin\delta - \frac{V_s^2}{2} \frac{x_{d\Sigma}' - x_{q\Sigma}}{x_{d\Sigma}' x_{q\Sigma}} \sin 2\delta - D\omega \right) \\ \quad -\frac{1}{T_a} m_g \\ \dot{m}_t = \left(a_0 a_2 b_3 - a_0 b_2\right) x_1 + \left(b_0 - a_1 b_2 - a_0 b_3 + a_1 a_2 b_3\right) x_2 \\ \quad + \left(b_1 - a_1 b_3 - a_2 b_3 + a_2^2 b_3\right) x_3 + \left(b_2 - a_2 b_3\right) y + \frac{b_3}{T_y}(u - y) \\ \dot{y} = \frac{1}{T_y}(u - y) \end{cases} \tag{13}$$

Where $b_0 = \frac{24 e_y}{e_{qh} h_w T_r^3}$, $b_1 = \frac{24 e e_y}{e_{qh} T_r^3}$, $b_2 = \frac{3 e_y}{e_{qh} h_w T_r}$ and $b_3 = \frac{e e_y}{e_{qh}}$.

And when the external load changes, the m_g usually changes accordingly in Eq. (13). Among them, adopting the parameters δ, ω, m_t and y as the state variables and selecting the parameters x_1, x_2 and x_3 as the intermediate variables.

III. Controller Design For HTRS System

In this section, the input/output feedback linearization control method is first used to design the sliding mode controller. Then, based on the design of traditional SMC controller, a novel idea is added to avoid the chattering phenomenon that caused by the traditional sliding mode control, which affects the control precision and control performance of the system, thus perfecting the design of the IPID-SMC controller.

A. Input/output Feedback Linearization Method

As can be seen from Eq. (13), there is no direct connection between the output of HTRS system ω and the output of controller u. Therefore, we differentiate the system output ω

with respect to time, and get the connection between ω and u is as follows.

$$\ddot{\omega} = f(x) + g(x) * u + d(t) \tag{14}$$

Where

$$f(x) = \frac{(a_0 a_2 b_3 - a_0 b_2)}{T_{ab}} x_1 + \frac{(b_0 - a_0 b_3 - a_1 b_2 + a_1 a_2 b_3)}{T_{ab}} x_2$$
$$+ \frac{(b_1 - a_1 b_3 - a_2 b_2 + a_2^2 b_3)}{T_{ab}} x_3 + (\frac{b_2}{T_{ab}} - \frac{a_2 b_3}{T_{ab}} - \frac{b_3}{T_{ab} T_y}) y$$
$$+ (\frac{-w_0 E_q' V_s}{x_{d\Sigma} T_{ab}} \cos\delta - \frac{w_0 V_s^2 (x_d' - x_q)}{x_d' x_q T_{ab}} \cos 2\delta + \frac{D^2}{T_{ab}^2}) \omega_t$$
$$+ \frac{D}{T_{ab}^2} (\frac{E_q' V_s}{x_{d\Sigma}} \sin\delta + \frac{V_s^2}{2} \frac{(x_d' - x_q)}{x_d' x_q} \sin 2\delta) - \frac{D}{T_{ab}^2} m_t$$

And $g(x) = \frac{b_3}{T_{ab} T_y}$.

B. Design of Traditional SMC Controller for HTRS System

There are two steps to design the SMC controller.

***Step*1**: Designing the sliding mode function $s(x)$.

In this paper, the sliding mode function is selected as:

$$s = \dot{e} + \lambda e \tag{15}$$

Where $e=\omega_d-\omega_t$, ω_d and ω_t denote the expected and actual output value of HTRS system, respectively. And e is the relative deviation of speed for HTRS system.

In order to improve the dynamic quality of approaching motion, the exponential approach law is used to ensure that when s is large, the system will approach the sliding mode state at a large speed. The expression of the exponential approach term is as follows.

$$\dot{s} = (\ddot{\omega}_d - \ddot{\omega}_t) + \lambda(\dot{\omega}_d - \dot{\omega}_t) = \eta * \mathrm{sat}(s) \tag{16}$$

Where λ, η are two positive constants, the saturation function sat(s) is an improvement on the basis of the sign function sgn(s), thus the sat(s) can be defined as follows.

$$\mathrm{sat}(s) = \begin{cases} 1, & s > \Delta \\ ks, & |s| \le \Delta, \quad k = 1/\Delta \\ -1, & s < -\Delta \end{cases} \tag{17}$$

Where Δ is a tiny number to ensure the saturation function owns a large slope.

***Step*2**: Designing the sliding control law u_{SMC}.

The equivalent sliding mode control is adopted in this paper. The equivalent sliding mode control is composed of an equivalent control item and a switching control item, which can be represented by Eq. (18). Among them, u_{eq} makes the state converge along the sliding mode surface when s is equal to 0; u_{sw} is used to force the state reaches the sliding surface, the switching item always works as long as the sliding mode surface is not equal to 0. The definitions of these two items can be denoted by Eq. (19) and (20).

$$u_{SMC} = u_{eq} + u_{sw} \tag{18}$$

$$u_{eq} = \frac{1}{g(x)} (\lambda * \dot{e} + \ddot{\omega} - f(x)) \tag{19}$$

$$u_{sw} = \frac{1}{g(x)} \eta \, \mathrm{sat}(s) \tag{20}$$

C. Design for the Improved PID-SMC Controller

In order to achieve the better performance of the nonlinear system, the robustness of the SMC controller and the good response characteristics of the PID controller are combined to design the PID-SMC controller. There are three main steps in the design of the improved PID-SMC controller (IPID-SMC).

***Step*1**: Designing the sliding mode function $s(x)$.

PID sliding mode is adopted to design the $s(x)$, and Lyapunov is used to prove the stability of the controller. What's more, the parameters K_p', K_i', K_d' of PID method is obtained through particle swarm optimization (PSO) algorithm. Therefore, the expressions of $s(t)$ and u_{eq} can be defined as follows.

$$s(t) = K_p' * e(t) + K_i' * \int e(t)dt + K_d' * \frac{de(t)}{dt} \tag{21}$$

According to literatures, the function of sliding mode surface can be defined as follows.

$$\dot{s}(t) = -\eta \, \mathrm{sgn}(s) - d(t) \tag{22}$$

Where K_p', K_i', K_d' are proportional, differential and integral adjustment parameters, respectively.

The expression of u_{eq} as Eq. (23) shows is obtained by deriving $s(t)$.

$$u_{eq} = \frac{1}{K_d' * g(x)} [K_p' * \dot{e} + K_i' * e + K_d' * \ddot{\omega} - K_d' * f(x)] \tag{23}$$

***Step*2**: Verifying the stability of system.

Corollary. For the model (13) about HTRS system, the system with the manifold (16) and control output (18) is stable in the sense of Lyapunov once the following two conditions are met.

(1) The system is controllable, i.e. $g(x) \not\equiv 0$.

(2) The external interference is bounded, i.e. $\exists \eta > D_r$, $D_r = \max_{t:0\to\infty} d(t)$.

Proof. A Lyapunov function is selected as Eq. (24) shows in this paper [19].

$$V(x) = \frac{1}{2} s^T s \tag{24}$$

The derivation of time is defined as follows.

$$\dot{V} = s\dot{s} = s(-\eta \, \mathrm{sgn}(s) - d(t)) = -\eta |s| - s \cdot d(t)$$
$$\le (-\eta - d(t))|s| \le 0 \tag{25}$$

Based on the asymptotic stability theorem, the sliding manifold is attractive and invariant [25], which is proved that the system is globally stable in the Lyapunov sense.

***Step*3**: Designing the switching function u_{sw}.

The switching function has a great influence on the degree of chattering for system. In order to eliminate chattering, the sign function is first replaced by the hyperbolic tangent function, which is continuous. And then add a trigonometric function term into the u_{sw}. The former embodies the dynamic quality when the system is close to the switching surface; the latter term reflects the dynamic quality when moving away from the switching surface. The combination of the two parts allows the system to smoothly reach the sliding surface from any state. Finally, the improved switch function can be described as follows.

$$u_{sw} = \frac{1}{g(x)} (\eta_1 * \tanh(\frac{s}{\xi})) + \eta_2 * \cos\beta \tag{26}$$

Where η_1, η_2 denote the convergence speed of HTRS system approaching to the sliding mode surface, ξ denotes the width of the boundary layer. And the value of these two parameters should be moderate, a higher value of η_1 and η_2 is likely to

generate chattering and a low value is likely to far away from the stable region. And the value of β is 3 in the literatures.

IV. Artificial Bee Colony Algorithm

In this paper, we proposed an improved artificial bee colony algorithm (IFABC) that combines the fuzzy control idea and the global optimal idea of PSO algorithm on the basis of ABC algorithm.

A. Standard Artificial Bee Colony Algorithm

In the nature, the behavior of bee colony searching for nectar source has been researched by more and more scholars. Specially, the artificial bee colony algorithm (ABC) is presented by Karaboga in 2005 [26]. In the process of foraging, different bees need to search for nectar source according to different division of labor and share search information to find a better nectar source, namely the optimal solution of the problem to be optimized. For the standard ABC algorithm, there are three stages and two kinds of behavior should be mentioned. These three stages include that employed bee phase, onlooker bee phase and scout bee phase, respectively. And two kinds of behavior include finding the new nectar sources and giving up the old nectar sources.

In a word, ABC algorithm is a commonly used intelligent optimization algorithm, which can be depicted as following three phases.

***Step* 1:** Initial phase

Initialize the location of the nectar source. In this paper, the positional component of the nectar source includes: ξ, η_1, η_2. The initial solution x_i（i=1,2,…,SN）is randomly generated at the beginning of the search. Therefore, the initial value of the j-th position component for the i-th nectar source in the neighborhood search range can be described as follows.

$$x_{i,j} = x_{i,j}^{\min} + rand(0,1)\left(x_{i,j}^{\max} - x_{i,j}^{\min}\right) \tag{27}$$

Where i=1,2,…,SN, and SN is the number of nectar source; j=1,2,…,D, D denotes the number of decision control variables. $x_{i,j}^{\max}$ and $x_{i,j}^{\min}$ are the upper and lower limits of the j-th position component, respectively.

***Step* 2:** Employed bee phase.

After starting the search, the employed bee searches for the nectar source that associated with it, and shares the corresponding nectar source information to the onlooker bee in the dance area through the swing dance. The new nectar source is searched by following equation.

$$v_{i,j} = x_{i,j} + \varphi_{i,j}\left(x_{i,j} - x_{k,j}\right) \tag{28}$$

Where i, $k \in \{1,2,\ldots,\mathrm{SN}\}$, $j \in \{1,2,\ldots,\mathrm{D}\}$, $\varphi_{ij} \in [-1,1]$. And k, j and φ_{ij} are generated randomly.

***Step* 3:** Onlooker bee phase

According to the information shared by employed bees, the onlooker bee selects the nectar source with higher fitness value as the new nectar source, which through the roulette mechanism. Moreover, the onlooker bee selects the nectar source would depend on the probability P_i, which can be calculated using the following equation.

$$P_i = \frac{Fit_i}{\sum_{j=1}^{SN} Fit_j} \tag{29}$$

Where P_i denotes the probability of the nectar source, Fit_i is the fitness value of the nectar source, which can be described as follows.

$$Fit_i = \begin{cases} \dfrac{1}{1+fit(x_i)} & if \;\; fit(x_i) \geq 0 \\ 1+\left|fit(x_i)\right| & if \;\; fit(x_i) < 0 \end{cases} \tag{30}$$

Where $fit(x_i)$ represents the objective function of the nectar source. What's more, the larger of the value of Fit_i, the greater probability that selecting the nectar source.

And the integral of time multiplied absolute error (ITAE) is first adopted as the objective function. Furthermore, in order to reduce the chattering and obtain better dynamic performance, the absolute error of the overshoot δ is added to the ITAE, which can be described as following equation.

$$fit(x_i) = \int_0^{T_i} \left(w_1 t\left|e(t)\right| + w_2 t\left|\delta(t)\right|\right) dt \tag{31}$$

Where w_1, w_2 represent the weight coefficient, T_i represents the integration time, $e(t)$ represents the error of the system, $\delta(t)$ represents the error of the overshoot.

It is worth mentioning that the greedy selection mechanism is used in the onlooker bee phase. Namely, if a nectar source with a higher fitness value is searched, the onlooker bee will convert into the employed bee for a new round of nectar collecting and information transfer.

***Step* 4:** Scout bee phase

If an employed bee is not found the higher fitness value until the *Limit* is reached, we will give up the nectar source. At the same time, the employed bee that associated with the nectar source is turned into a scout bee. The search equation can be described as follows.

$$x_{i,j} = x_{i,j}^{\min} + rand(0,1)\left(x_{i,j}^{\max} - x_{i,j}^{\min}\right) \tag{32}$$

B. Improved Fuzzy Artificial Bee Colony Algorithm

There may be some shortcomings such as slow convergence speed and poor convergence precision from the ABC algorithm. Therefore, we proposed an improved ABC algorithm to optimize the parameters of controllers.

Improvement 1: Global optimization search strategy.

In order to ensure better development and utilization of nectar source, the global-best (*g-best*) idea that came from particle swarm optimization (PSO) is added into the standard ABC algorithm in the phase of employed and onlooker bees. The new search equation is as follows.

$$v_{i,j} = x_{i,j} + \varphi_{i,j}\left(x_{i,j} - x_{k,j}\right) + r_{i,j}\left(x_{g-best} - x_{i,j}\right) \tag{33}$$

Where x_{gbest} denotes the global optimal value of the current j-th element; $r_{i,j}$ is a random number between 0 and 1.5 [27]. The update section *g-best* could drive the pending optimization solution to be globally optimal, and avoid the algorithm falling into local optimum and premature convergence.

Improvement 2: Scout bee adaptive search strategy.

In the stage of scout bees, the new position of the scout bees is randomly generated, namely the position is uncertain. Therefore, the process can be treated as a fuzzy process. The adjustment of scout bees´ position p is introduced in the process [28], and the equation of p can be depicted as follows.

$$p = p_{\max} - \frac{\text{Iteration}}{\text{MaxCycle}}\left(p_{\max} - p_{\min}\right) \tag{34}$$

Where MaxCycle denotes the maximum number of iterations, $p_{\max}$ and $p_{\min}$ denotes the maximum and minimum of position adjustment percentage p.

It can be obtained from the literature [28] that the values of $p_{\max}$ and $p_{\min}$ are 1 and 0.2, respectively, indicating that the

adjustment position adjustment percentage based on the current position of the scout be reduced linearly from 100% to 20% in each round of experiments. However, the linearly reduced position adjustment percentage has some defects, such as the search range is small at the later stage of the search and the scout bee has converged to the vicinity of the optimal value. What's more, the smaller the search range, the more easily the scout bee falls into the local optimum. Therefore, the position adjustment percentage that is nonlinear and dynamic as shown in Eq. (34) is adopted.

At the same time, in order to solve the problem of the value of the p in different iteration periods, the fuzzy control idea is introduced to further improve the ABC algorithm. Among them, the position adjustment percentage correction value p_c is affected by two factors: the current position adjustment percentage p and the current bee population optimal nectar source quality *NCValue*, which is defined as follows.

$$NCValue = \frac{Value - Value_{\min}}{Value_{\max} - Value_{\min}} \tag{35}$$

Where $Value_{\max}$ denotes the maximum nectar source quality of the initial bee colony, namely the maximum fitness value; $Value_{\min}$ and *Value* denote the final and optimal nectar source quality of the current bee colony, respectively.

In the fuzzy control, *NCValue* and p are taken as the fuzzy control input, and the output of the fuzzy control is the position adjustment percentage correction value p_c, and the design of the fuzzy rule should satisfy the following conditions.

1) At the beginning of the iteration, p is larger. If *NCValue* is large, it means that the scout bee is far from the optimal value, thus it is necessary to expand the search range so that the scout bee can fully explore in global scope. If *NCValue* is at a medium or small value, it means that the scout bee is closer to the optimal value, and the search range needs to be narrowed appropriately, thus the p_c should take a medium or small value.
2) In the middle of the iteration, p is moderate. If *NCValue* is large or medium, p_c should take a medium value. If *NCValue* is small, namely the scout bee is extremely close to the optimal value, in order to drive the scout bee performs a fine search near the optimal value, p_c should take a smaller value.

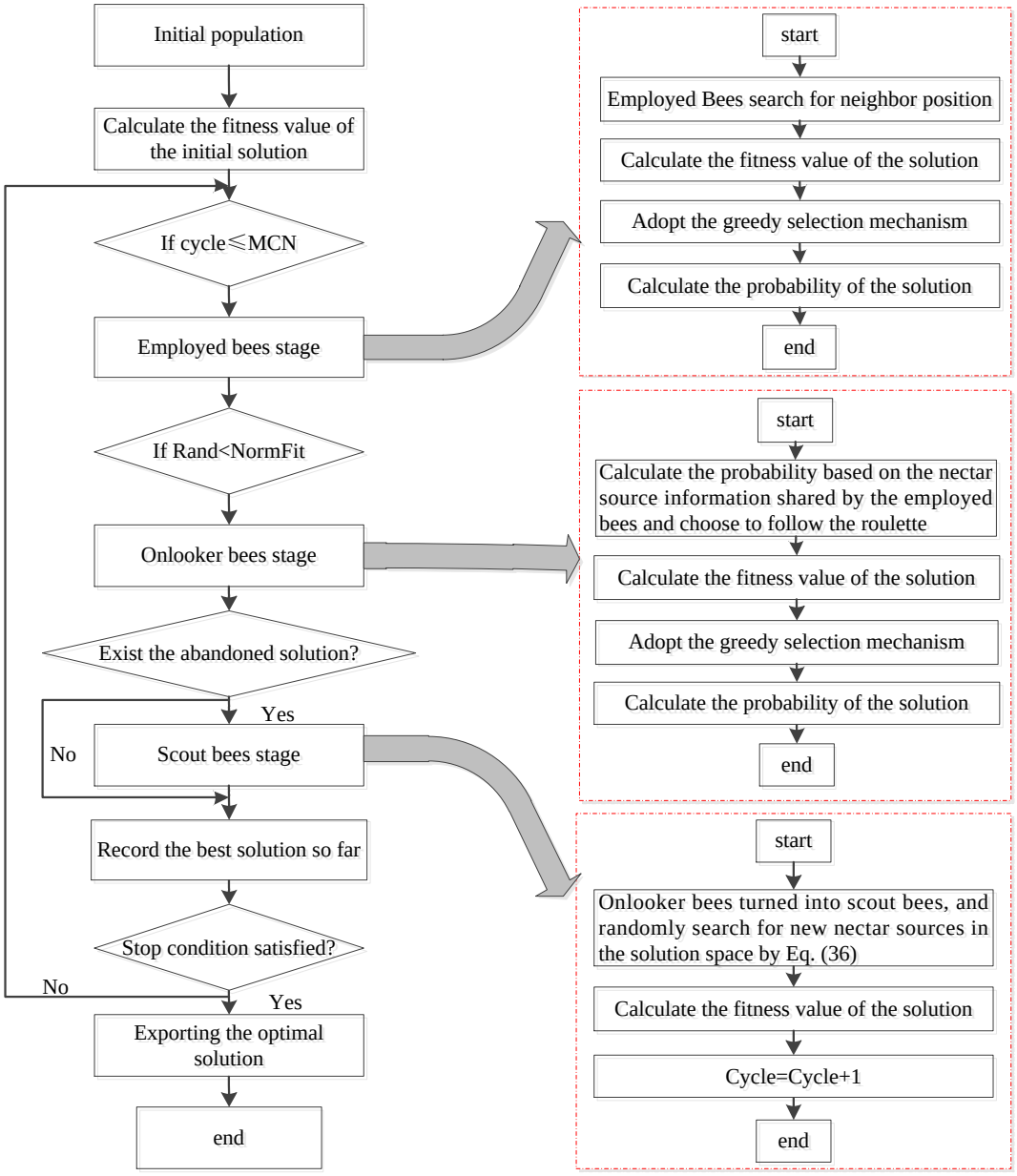

Fig. 3.The flow chart of improved fuzzy artificial bee colony algorithm (IFABC)

3) At the end of the iteration, p is small. If *NCValue* is large or medium, in order to expand the search range for the scout bee, p_c should be taken large.

In a word, the fuzzy rule of p_c is shown in TABLE I. The input and output adopt small (S), medium (M) and large (L) as the fuzzy sets.

TABLE I
THE FUZZY CONTROL RULES TABLE

p_c / p / *NCValue*	S	M	B
S	M	S	S
M	B	M	M
B	B	M	B

The improved search equation for the scout bee can be described as follows.

$$v_{i,j} = x_{i,j} + rand(0,1)\, p_c x_{i,j} \tag{36}$$

In the Eq. (36), the search space of the scout bee changes nonlinearly with the number of iterations.

In summary, the flow chart of the IFABC algorithm is shown in Fig. 3. The pseudo-code of IFABC algorithm is given in TABLE II below.

V. PARAMETERS OPTIMIZATION OF IPID-SMC CONTROLLER BASED ON IFABC ALGORITHM

For the improved PID-SMC controller, this paper completes the design by optimizing following parameters. The expression of s is defined as Eq. (23). It can be seen the values of K_p', K_i', K_d' have a great influence on the sliding mode approach law, thus the PSO algorithm is adopted to optimize the parameters of PID control. The factors η_1, η_2, ξ are to be optimized by IFABC algorithm. In addition, η_1 and η_2 will affect degree of chattering of the IPID-SMC controller, and the smallest ξ may cause the great approximation in the control process.

Based on the above discussion, the parameters of the IPID-SMC to be optimized by the PSO and IFABC algorithm can be depicted as $\theta_1=[K_p', K_i', K_d']$, $\theta_2=[\eta_1, \eta_2, \xi]$, respectively. The structure scheme of the IPID-SMC controller optimized by proposed IFABC algorithm is shown in Fig. 4.

VI. NUMERICAL SIMULATIONS AND DISCUSSIONS

In this section, a series of simulations are executed for HTRS system. The mathematical simulation model of HTRS system is carried out when it is under unload and load conditions. The step signal is taken as the tracking signal, and the dynamic characteristics of the HTRS system are judged by

TABLE II
PSEUDO CODE OF IFABC ALGORITHM

Input: objective function: $f(x)$,$x=[x_1,x_2,\ldots,x_{SN}]^T$
Begin
Set the control variable dimension D, the population size SN, the number of maximum cycles MCN and the control parameter $Limit$
Calculate the fitness value of the initial solution $f(x_i)$
Set $trial(i) = 0$ and $cycle = 1$, where $i = 1,2,\ldots,SN$
//$trial(i)$ denotes the unimproved number of the solution x_i
//$cycle$ denotes the iteration of algorithm
if $cycle \le MCN$ **then**
//The employed bees phase
for i=1 to SN **do**
Produce a new candidate nectar source v_i for the employed bee corresponding to food source x_i using Eq.(33). Where the global best (g-$best$) idea is added into the Eq.(28)
//Select the better one between v_i and x_i
if $f(v_i)<f(x_i)$ **then**
Replace solution x_i with candidate solution v_i and named as x_{best}
Set $trial(i) = 0$
else
Set $trial(i) = trial(i) + 1$
end for
Calculate the fitness values of nectar sources and probability p_i by using Eq.(29)
//The onlooker bees phase
Set $t = 0$, $i = 1$
while $t < SN$ **do**
if $rand < p_i$ **then**
Set $t = t + 1$
Repeat the operation of employed bees phase
end if
Set $i = i+ 1$ and **if** $i > SN$ **then** $i = 1$
end while
// The scout bees phase
for $i = 1$ to SN **do**
if $trial(i) \ge Limit$ **then**
Introduce variable P_c and search for it according to Eq.(36)
end if
end for
Set $cycle = cycle + 1$
end if
End
output: x_{best} and $f(x_{best})$

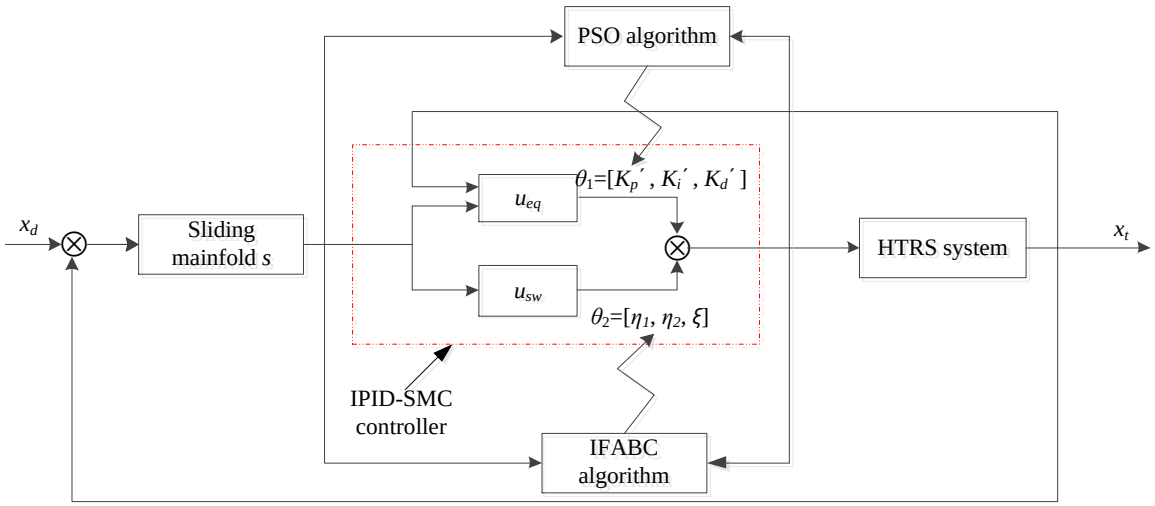

Fig. 4.The structure scheme of the IPID-SMC controller optimized by IFABC algorithm

observing the state of the step output response of HTRS system. The simulation time is set as 30s and the simple time is set as 0.01s. And some parameters of HTRS system are set as TABLE III.

TABLE III
THE PARAMETER SETTINGS OF HTRS SYSTEM

Parameters	Values	Parameters	Values
W_0	314.0	V_s	1.000
T_{ab}	8.000	e_{qh}	0.500
D	0.500	e_y	1.000
E'_q	1.350	e_m	0.700
$x_d{}'_\Sigma$	1.150	T_r	1.000
$x_q{}'_\Sigma$	1.474	h_w	2.000
T_y	0.100		

A. Comparison of Controllers

In order to verify the superiority of the designed IPID-SMC controller, the PID controller, standard SMC controller and IPID-SMC controller are adopted in the HTRS system, respectively. The parameters of the three controllers are optimized by the IFABC algorithm, and the parameter settings of the IFABC algorithm are shown in TABLE IV. It is worth mentioning that the parameter determination of IPID-SMC controller is set as: $\theta_{IPID\text{-}SMC} = [\eta_1, \eta_2, \xi]$, and the parameters of IPID-SMC controller that include K_p' , K_i' and K_d' will get through the PSO algorithm, namely $K_p' = 3.2597$, $K_i' = 0.2941$, $K_d' = 2.5815$ (K_p' , K_i' and K_d' denote the proportional, integral and differential coefficients of IPID-SMC controller, respectively).

On the problem of designing the controller for HTRS system, the proposed IPID-SMC controller performed well compared to other controllers. As shown in Fig. 5, it can be seen from the step response of HTRS system between PID controller, SMC controller and IPID-SMC controller. From the TABLE V, we can know the IPID-SMC controller achieves the shorter rise time, shorter settling time and smaller overshoot compared to PID controller, and the rise time, settling time and overshoot are reduced by 52.80%, 32.77% and 62.22%, respectively. And compared with SMC controller, IPID-SMC controller has the longer settling time, but achieves the shorter rise time and smaller overshoot than SMC controller, the rise time and overshoot of IPID-SMC controller is reduced by 39.02% and 55.93% compared with SMC controller, respectively.

TABLE IV
PARAMETERS SETTING FOR IFABC ALGORITHM

Parameters	Values	Parameters	Values
Population	30	$p_{\min}$	0.2
MaxCycle	100	w_1	1
Limit	100	w_2	100
$Value_{\max}$	20	$\omega_{\max}$	0.9
$Value_{\min}$	10	$\omega_{\min}$	0.02
$CBPE_{\max}$	30	$x_{\max}$	30
$CBPE_{\min}$	10	$x_{\min}$	0
$p_{\max}$	1		

Similarly, the step response of HTRS system between three controllers is shown in Fig. 6 when it is under the load condition. As TABLE VI shows, compared with the PID controller, the IPID-SMC controller achieves the shorter rise time, shorter settling time and smaller overshoot that are reduced by 28.57%, 68.40% and 96.56%, respectively. Compared with the standard SMC controller when it is under the load condition, the IPID-SMC controller possesses longer rise time and settling time, but the overshoot is reduced by 84.11%.

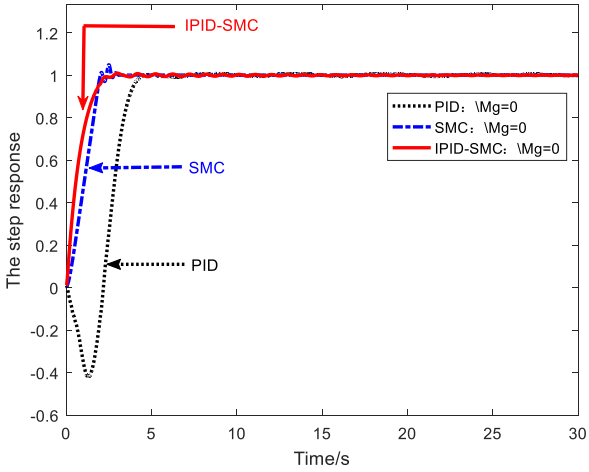

Fig. 5.The step response of HTRS system under unload condition

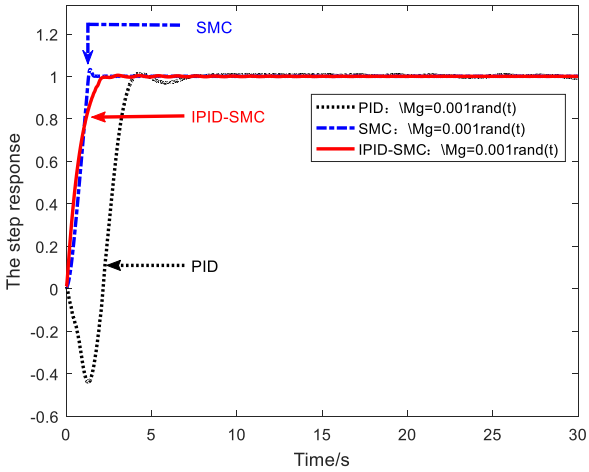

Fig. 6.The step response of HTRS system under load condition

TABLE V
THE COMPARISON OF DYNAMIC PERFORMANCE FOR DIFFERENT CONTROLLERS (Mg=0)

Controllers	PID controller	SMC controller	IPID-SMC controller
Rise time (t_r)	4.47	3.46	2.11
Settling time (t_s)	4.15	2.08	2.79
Overshoot	0.011579	0.009924	0.004374

TABLE VI
THE COMPARISON OF DYNAMIC PERFORMANCE FOR DIFFERENT CONTROLLERS (Mg=0.001rand(t))

Controllers	PID controller	SMC controller	IPID-SMC controller
Rise time (t_r)	3.92	1.40	2.80
Settling time (t_s)	6.17	1.48	1.95
Overshoot	0.023237	0.005034	0.000800

In a word, compared with the others, the IPID-SMC controller that proposed in this paper gets the better dynamic performance for HTRS system.

B. Comparison of Optimization Algorithm

According to the comparison of several controllers in the above sections, the effect of tracking step response and dynamic performance of the IPID-SMC controller proposed

in this paper are better than those of the PID controller and standard SMC controller. Therefore, different optimization algorithms that including DE algorithm, PSO algorithm, ABC algorithm and IFABC algorithm will be used to optimize the parameters of the IPID-SMC controller. What's more, the parameters setting for IFABC algorithm are shown in the TABLE IV.

In order to verify the superiority of IFABC algorithm that optimizing the parameters of IPID-SMC controller and the dynamic performance of HTRS system, the simulation experiment of HTRS system that under unload and load conditions were carried out. When it is under the unload condition, the convergence curve of the fitness function are shown in Fig. 7. And the process of tracking the step response is also shown in Fig. 8. The comparison of experimental results between the DE algorithm, PSO algorithm, ABC algorithm and the proposed IFABC algorithm are shown in TABLE VII.

On the problem of parameter optimization of IPID-SMC controller for the HTRS system, the proposed IFABC algorithm performed well in convergence speed and convergence accuracy when it is compared to all other algorithms, which include DE algorithm, PSO algorithm and ABC algorithm in this paper.

As shown in Fig. 7 and Fig. 9, it can be seen from the distribution of the average optimal value that compared with DE algorithm, PSO algorithm and ABC algorithm, we can see IFABC algorithm achieves better convergence speed and convergence precision whether in the unload(Mg=0) and load(Mg=0.001rand(t)) conditions. For example, IFABC algorithm has smaller overshoot and shorter settling time than other four algorithms when it is under the unload(Mg=0) condition. Analyzing in more detail, the settling time of IFABC algorithm is reduced by 19.07% and 6.73% compared with DE algorithm and ABC algorithm, respectively. Similarly, we can find that IFABC algorithm could find the smallest *BestJ* (the best solution), the value of *BestJ* is reduced by 27.08%, 0.36% and 5.47% when it is compared with DE algorithm, PSO algorithm and ABC algorithm, respectively.

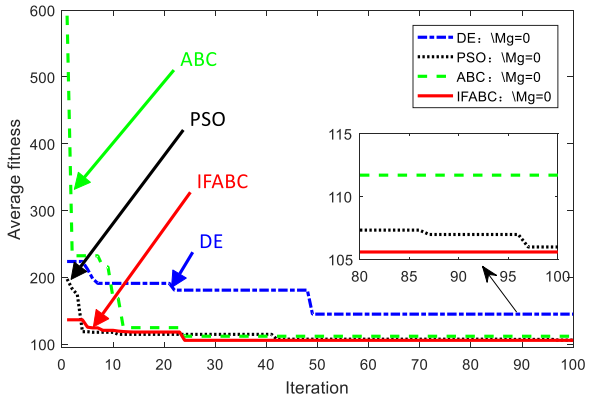

Fig. 7.The average curve of fitness function (Mg=0)

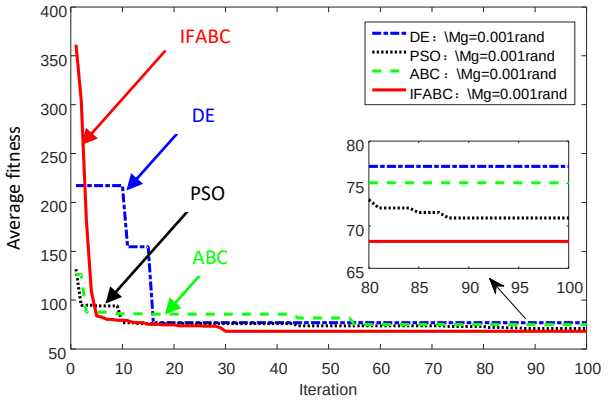

Fig. 9.Average curve of fitness function (Mg=0.001rand(t))

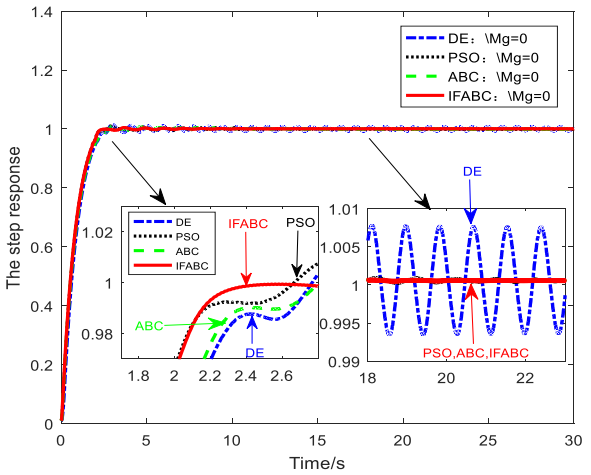

Fig. 8.The step response of HTRS system (Mg=0)

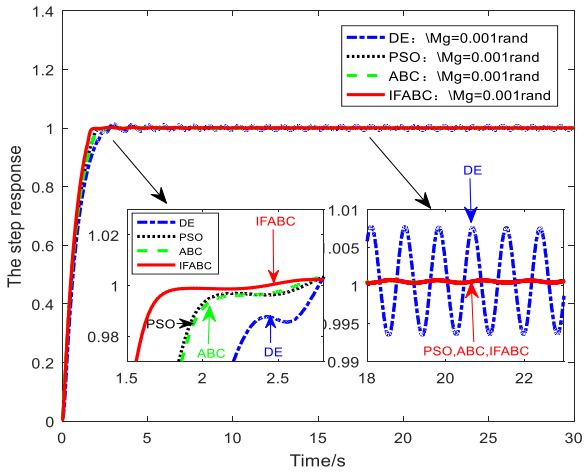

Fig. 10.Step response of HTRS (Mg=0.001rand(t))

TABLE VII
SIMULATION RESULTS COMPARISON OF DIFFERENT ALGORITHM FOR HTRS SYSTEM (Mg=0)

Algorithms	DE	PSO	ABC	IFABC
BestJ	144.7939	105.96337	111.6881	105.5778
Overshoot	0.009137	—	0.010353	0.004374
t_s(s)	2.570000	>30.00000	2.230000	2.080000
η_1	7.649211	15.96337	20.99314	30.00000
η_2	-0.66234	0.047398	-0.52896	0.017976
ξ	0.283131	1.104583	1.192439	2.060124

TABLE VIII
SIMULATION RESULTS COMPARISON OF DIFFERENT ALGORITHM FOR HTRS SYSTEM (Mg=0.001rand(t))

Algorithms	DE	PSO	ABC	IFABC
BestJ	75.08365	70.94592	77.01785	68.17113
Overshoot	0.026161	—	0.003712	0.001841
t_s(s)	13.13000	>30.00000	1.910000	1.590000
η_1	10.61311	13.41933	30.00000	27.57661
η_2	-1.31742	0.61367	0.553908	1.211420
ξ	0.479163	1.167796	2.472420	3.931905

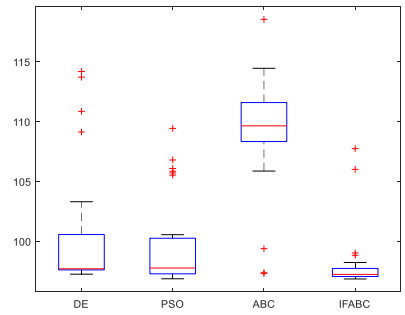

Fig. 11.The boxplot of four algorithms for PID controller

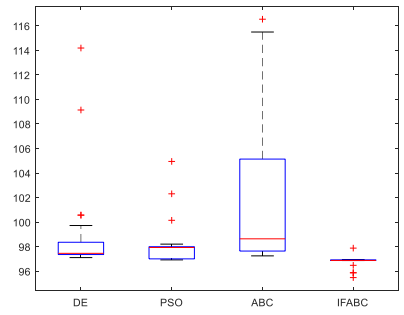

Fig. 12.The boxplot of four algorithms for SMC controller

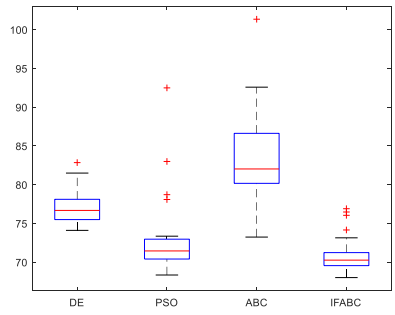

Fig. 13.The boxplot of four algorithms for IPID-SMC controller

TABLE IX
THE MEAN AND STANDARD DEVIATION OF FOUR ALGORITHMS FOR THREE CONTROLLERS

Function	Controller	DE		PSO		ABC		IFABC	
		Mean	Std	Mean	Std	Mean	Std	Mean	Std
$fit(x_i)$	PID	97.2567	4.867028	99.75927	3.594655	109.2909	4.517297	98.03619	2.433604
	SMC	98.77722	3.630220	98.01765	1.672516	101.4619	5.529848	96.79157	0.406455
	PID-SMC	77.19470	2.07406	72.76965	4.718282	83.27882	5.687904	70.84851	2.265957

Similarly, Fig. 9 and Fig. 10 shown the average curve and the step response of HTRS system when it is under the load condition.

As TABLE VIII shows, IFABC algorithm has smaller overshoot and shorter settling time than other four algorithms when it is under the load condition, the settling time of IFABC algorithm is reduced by 88.78% and 16.75% compared with DE algorithm and ABC algorithm, respectively. At the same time, we can find that IFABC algorithm could obtain the smallest *BestJ* (the best solution), the value of *BestJ* is reduced by 47.55%, 11.00% and 12.16% when it is compared with DE algorithm, PSO algorithm and ABC algorithm, respectively.

C. Algorithm Comparison of Different Controllers

In this paper, we have performed 30 independent operations for these four algorithms. The contents of the above analysis are only the best simulation results for the 30 operations of these four algorithms. Therefore, this section will calculate the results of 30 operations of these four algorithms and illustrate with boxplots, which illustrate the statistical data of the minimum objective value (*BestJ*), reflecting the distribution of the indicator data of the four algorithms and the comparison of the distribution characteristics. As for the PID controller, SMC controller and IPID-SMC controller, the boxplots for *BestJ* of them about four algorithms are shown in Fig. 11, Fig. 12 and Fig. 13, respectively.

As Fig. 11 shows, the IFABC algorithm that applied in the PID controller has the lowest *BestJ* value, the best overall level, and a more uniform distribution when it is compared with other algorithms, which include DE algorithm, PSO algorithm, and ABC algorithm.

Similarly, the proposed IFABC algorithm also possesses the smaller *BestJ* value, more even distribution and better overall level for SMC controller and the proposed IPID-SMC controller. At the same time, as can be seen from the comparison of the three figures, the IPID-SMC controller also has the smallest *BestJ*.

In order to further observe the performance of the above indicators, TABLE IX shows the mean and standard deviation values of the objective function. As seen in the TABLE IX, from the perspective of the algorithm, the mean value and standard deviation values of the IFABC algorithm are better than those other four algorithms. It is also indicates that IFABC algorithm has certain competitive advantages and can obtain solutions with better diversity. From the perspective of the controller, it also can be seen from the TABLE IX that the IPID-SMC controller has the better performance than other controllers.

According to above discussion and analysis, it is can be seen that the IFABC-based IPID-SMC controller could get the best transient process and dynamic performance whether the HTRS system under unload and load conditions.

VII. CONCLUSIONS

In this paper, a novel controller has been proposed for the nonlinear HTRS system by combining the sliding mode control and PID control strategy. The simulation results indicate that the proposed IPID-SMC controller outperforms than PID controller and traditional SMC controller in tracking step effects and reducing chattering. Furthermore, the challenge of parameter optimization of IPID-SMC controller is studied, namely an improved fuzzy artificial bee colony algorithm (IFABC) is proposed by combining the global optimal and fuzzy control thought based on the standard ABC algorithm. The simulation results indicate that the proposed IFABC algorithm outperforms DE algorithm, PSO algorithm and ABC algorithm in convergence speed and convergence accuracy whether under unload condition and uncertain load conditions.

In summary, the proposed IPID-SMC controller that based on the improved fuzzy artificial bee colony algorithm has been applied to adjust the nonlinear HTRS system could get the fine hydraulic transient process and great dynamic performance.

ACKNOWLEDGMENT

The authors would like to thank the editors and the reviewers for their constructive comments and suggestions. This work is supported by Innovation Team Program of Chongqing Education Committee (CXTDX201601019), Chongqing University Innovation Team under Grant

(KJTD201312) and the National Natural Science Foundation of China (Nos. 51207064 and 61463014).

REFERENCES

[1] B. Xu, D. Chen, H. Zhang, and F. Wang, "Modeling and stability analysis of a fractional-order Francis hydro-turbine governing system," *Chaos Solitons & Fractals*, vol. 75, pp. 50-61, 2015.

[2] W. Yang, P. Norrlund, J. Bladh, J. Yang, and U. Lundin, "Hydraulic damping mechanism of low frequency oscillations in power systems: Quantitative analysis using a nonlinear model of hydropower plants," *Applied Energy*, vol. 212, pp. 1138-1152, 2018.

[3] D. Chen, C. Ding, X. Ma, P. Yuan, and D. Ba, "Nonlinear dynamical analysis of hydro-turbine governing system with a surge tank," *Applied Mathematical Modelling*, vol. 37, pp. 7611-7623, 2013.

[4] F. Wang, D. Chen, B. Xu, and H. Zhang, "Nonlinear dynamics of a novel fractional-order Francis hydro-turbine governing system with time delay," *Chaos Solitons & Fractals*, vol. 91, pp. 329-338, 2016.

[5] W. Su, C. E. Lin and C. Huang, "Hybrid filter application for power quality improvement," *Electric Power Systems Research*, vol. 47, pp. 165-171, 1998.

[6] W. Zhu, Y. Zheng, J. Dai, and J. Zhou, "Design of integrated synergetic controller for the excitation and governing system of hydraulic generator unit," *Engineering Applications of Artificial Intelligence*, vol. 58, pp. 79-87, 2017.

[7] H. Liang, H. Zhang and Z. Wang, "Distributed-observer-based cooperative control for synchronization of linear discrete-time multi-agent systems," *ISA Transactions*, vol. 59, pp. 72-78, 2015.

[8] R. Vilanova and O. Arrieta, "PID design for improved disturbance attenuation: min max Sensitivity matching approach," *IAENG International Journal of Applied Mathematics*, vol. 37, no.1, pp. 33-39, 2007.

[9] H. Feng, C. Yin, W. Ma, H. Yu, and D. Cao, "Parameters identification and trajectory control for a hydraulic system," *ISA Transactions*, 2019.

[10] K. Lu, W. Zhou, G. Zeng, and W. Du, "Design of PID controller based on a self-adaptive state-space predictive functional control using extremal optimization method," *Journal of the Franklin Institute*, vol. 355, pp. 2197-2220, 2018.

[11] S. A. Misal and V. S. Sathe, "Application of proposed improved relay tuning for design of optimum PID control of SOPTD model," *Arpn Journal of Systems & Software*, pp. 246-250, 2012.

[12] F. O. Arteaga, D. G. Buitrago and E. Giraldo, "Sliding mode control applied to MIMO system," *Engineering Letters*, vol. 27, no.4, pp. 802-806, 2019.

[13] H. Zhang, M Du and W. Bu, "Sliding mode controller with RBF neural network for manipulator trajectory tracking," *IAENG International Journal of Applied Mathematics*, vol. 45, no.4, pp. 334-342, 2015.

[14] X. Ding and A. Sinha, "Hydropower plant load frequency control via second-order sliding mode," *Journal of Dynamic Systems, Measurement, and Control*, vol. 139, pp. 653-659, 2017.

[15] N. Cibiraj and M. Varatharajan, "Chattering reduction in sliding mode control of quadcopters using neural networks," *Energy Procedia*, vol. 117, pp. 885-892, 2017.

[16] B. M. Al-Hadithi, A. J. Barragán, J. M. Andújar, and A. Jiménez, "Chattering-free fuzzy variable structure control for multivariable nonlinear systems," *Applied Soft Computing*, vol. 39, pp. 165-187, 2016.

[17] G. K. E. and A. J., "Control of nonlinear two-tank hybrid system using sliding mode controller with fractional-order PI-D sliding surface," *Computers & Electrical Engineering*, vol. 71, pp. 953-965, 2018.

[18] M. Vijay and D. Jena, "PSO based neuro fuzzy sliding mode control for a robot manipulator," *Journal of Electrical Systems and Information Technology*, vol. 4, pp. 243-256, 2017.

[19] Z. Chen, X. Yuan, Y. Yuan, X. Lei, and B. Zhang, "Parameter estimation of fuzzy sliding mode controller for hydraulic turbine regulating system based on HICA algorithm," *Renewable Energy*, vol. 133, pp. 551-565, 2019.

[20] A. Yurtkuran and E. Emel, "An enhanced artificial bee colony algorithm with solution acceptance rule and probabilistic multisearch," *Computational Intelligence and Neuroscience*, vol. 1, pp. 1-13, 2016.

[21] J. Wang and J. Song, "A hybrid algorithm based on gravitational search and particle swarm optimization algorithms to solve function optimization problems," *Engineering Letters*, vol. 25, no.1, pp. 22-29, 2017.

[22] S. Li, L. Jiao, Y. Zhang, Y. Wang, and W. Sun, "A scheme of resource allocation for heterogeneous services in peer-to-peer networks using particle swarm optimization," *IAENG International Journal of Computer Science*, vol. 44, no.4, pp. 482-488, 2017.

[23] G. Chen, Z. Lu, Z. Zhang, and Z. Sun, "Research on hybrid modified cuckoo search algorithm for optimal reactive power dispatch problem," *IAENG International Journal of Computer Science*, vol. 45, no.2, pp. 328-339, 2018.

[24] S. Li and J. Wang, "Improved cuckoo search algorithm with novel searching mechanism for solving unconstrained function optimization problem," *IAENG International Journal of Computer Science*, vol.44, no.1, pp.8-12, 2017.

[25] X. Yuan, Z. Chen, Y. Yuan, Y. Huang, X. Li, and W. Li, "Sliding mode controller of hydraulic generator regulating system based on the input/output feedback linearization method," *Mathematics and Computers in Simulation*, vol. 119, pp. 18-34, 2016.

[26] D. Karaboga and B. Akay, "A comparative study of artificial bee colony algorithm," *Applied Mathematics and Computation*, vol. 214, pp. 108-132, 2009.

[27] G. Zhu and S. Kwong, "Gbest-guided artificial bee colony algorithm for numerical function optimization," *Applied Mathematics and Computation*, vol. 217, pp. 3166-3173, 2010.

[28] A. Banharnsakun, T. Achalakul and B. Sirinaovakul, "The best-so-far selection in artificial bee colony algorithm," *Applied Soft Computing*, vol. 11, pp. 2888-2901, 2011.